An Algorithm for the In-Field Calibration of a MEMS IMU

Umar Qureshi and Farid Golnaraghi

***Abstract*— Recently, micro electro-mechanical systems (MEMS) inertial sensors have found their way in various applications. These sensors are fairly low cost and easily available but their measurements are noisy and imprecise, which poses the necessity of calibration. In this paper, we present an approach to calibrate an inertial measurement unit (IMU) comprised of a low-cost tri-axial MEMS accelerometer and a gyroscope. As opposed to existing methods, our method is truly infield as it requires no external equipment and utilizes gravity signal as a stable reference. It only requires the sensor to be placed in approximate orientations, along with the application of simple rotations. This also offers easier and quicker calibration comparatively. We analyzed the method by performing experiments on two different IMUs: an in-house built IMU and a commercially calibrated IMU. We also calibrated the in-house built IMU using an aviation grade rate table for comparison. The results validate the calibration method as a useful low-cost IMU calibration scheme.**

***Index Terms*— Accelerometer and gyroscope calibration, inertial measurement unit (IMU), micro electro-mechanical systems (MEMS), multi-position calibration, gravity based in-field calibration, low cost IMU calibration.**

I. Introduction

RECENT development in MEMS technology has enabled low cost, low power and small sized sensors to be manufactured. These sensors have been adopted into various applications including navigation and positioning, medical electronics and teaching systems [1]–[3]. Potential use of MEMS sensors in user interfaces have also been explored by researchers over some time [4]–[6].

MEMS sensors offer benefits in ways mentioned above, but their measurements are not accurate as their tactical grade counterparts and suffer from bias, noise, scaling errors, non-linearity, temperature based variations and misalignment errors. It is evident that significant accuracy can only be derived from these sensors if their errors are properly compensated by a calibration scheme.

Calibration is the process of comparing instrument outputs with known reference information and determining the coefficients that force the output to agree with the reference information over a range of output values [7]. Conventionally, the calibration of navigation grade inertial sensors is done by using mechanical platforms and rate tables, which rotate the device to precisely controlled orientations and rotation rates [8]. However, these are expensive and require a controlled environment, which makes them economically unfeasible and unsuitable for MEMS sensors calibration.

To overcome the difficulty associated with using expensive mechanical platforms, alternate calibration methods have been explored by researchers over time. Ferraris *et al.* [9] proposed an in-filed calibration method for accelerometer and a gyroscope. They calibrated the accelerometer using gravity based 6-position method. They carefully constructed the sensor case to allow for perfect alignments of the sensor with gravity. They calibrated the bias of gyro by using static intervals and for the scale and misalignments, they performed complete rotations around each axis. To perform the rotations, their method required an external reference block, which only allowed 2 different rotations to be applied. Skog and Händel [10] proposed a calibration method for both an accelerometer and a gyroscope. Their calibration method for the accelerometer utilizes gravity as a reliable external reference and does not require the sensor to be placed in special orientations. For the gyroscope's calibration, they proposed the use of a turntable; however, the actual calibration of the gyroscope was not shown in the paper. Syed *et al.* [11] analyzed the problem of INS calibration for GPS integration. They modified the gravity based multi-position calibration method, originally described in [12], with the inclusion of approximate up and down configurations for the removal of large biases from the accelerometer. They further modified the method by utilizing a single-axis turntable instead of using Earth's rotation rate for the calibration of the gyroscope, since it is very weak to be detected by a MEMS gyro. Jurman *et al.* [13] calibrated an IMU in-field with a combination of the gravity based accelerometer calibration method and the gyro calibration method of [9]. Olivares *et al.* [14] proposed a modified method to eliminate the need of a turntable for the gyroscope's calibration. Their approach was to calibrate the accelerometer first using the gravity based 6-position method and then use a combination of the calibrated accelerometer and a bike wheel to calibrate the gyroscope.

For the case of an accelerometer, the gravity based methods do eliminate the dependence on external equipment and hence, can be carried out easily in the field. On the other hand, the use of a turntable or any other external equipment for gyroscope's calibration not only limits the true in-field calibration of the sensor but increases the overall costs as well.

With the ongoing development in MEMS technology, the manufacturers of inertial sensors are aiming more toward combining different sensors on a single chip so as to reduce size and cost even more, for example, the sensor we used:

Manuscript received July 11, 2017; revised August 24, 2017; accepted August 27, 2017. Date of publication September 12, 2017; date of current version October 24, 2017. This work was supported by the Natural Sciences and Engineering Research Council of Canada. The associate editor coordinating the review of this paper and approving it for publication was Prof. Octavian Postolache. *(Corresponding author: Farid Golnaraghi.)*

The authors are with the Mechatronic System Engineering, Simon Fraser University, Surrey, BC V3T 0A3, Canada (e-mail: mqureshi@sfu.ca; mfgolnar@sfu.ca).

Digital Object Identifier 10.1109/JSEN.2017.2751572

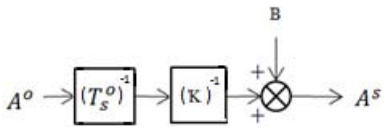

Fig. 1. Sensor model with gain, misalignment matrix and bias.

BNO055 by Bosh, combines an accelerometer, a gyroscope and a magnetometer on a single chip. As these new single-chip, low cost and multi-sensor devices find more applications in the future, cheaper methods of calibration or ideally methods with zero additional cost would be much more practical.

In this paper, we propose a calibration algorithm for low cost IMUs that can be executed without any external equipment in-field. The method is also simpler in terms of both physical application and required computations. The organization of the paper is as follows. In section II, the sensor error model is derived. In section III, the calibration method is described. Results are discussed in Section IV and conclusion is drawn in section V.

II. Sensor Error Model

A. Tri-Axial Accelerometer

Ideally in a tri-axial accelerometer, all three sensing axes should be orthogonal to each other. However, in a practical sensor, small non-orthogonalities may exist between the sensing axes due to manufacturing limitations. To account for these non-orthogonalities, we will assign a perfectly orthogonal coordinates axis to the body of the sensor.

As shown in [10], assuming that the misalignment between the orthogonal body axes and the non-orthogonal sensor axes is small, the force measured by the accelerometer in sensor (non-orthogonal) coordinates can be transformed into orthogonal body coordinate axes as;

$$\mathrm{A}^o = \left(\mathrm{T}_\mathrm{s}^o\right)^{-1} \mathrm{A}^\mathrm{s} \tag{1}$$

Where T_s^o is,

$$\left(\mathrm{T}_\mathrm{s}^o\right)^{-1} = \begin{bmatrix} 1 & -\theta_{yz} & \theta_{zy} \\ \theta_{xz} & 1 & -\theta_{zx} \\ -\theta_{xy} & \theta_{yx} & 1 \end{bmatrix} \tag{2}$$

Where A^s is the force measured in the accelerometer's coordinates, A^o is the force in orthogonal body coordinates and T_s^o is the rotation matrix describing the correction rotations.

By assuming that the sensor axis x^s aligns with the body axis x^o and that the axis y^s lies in the plane formed by x^o and y^o axes, the angles θ_{xz}, θ_{xy} and θ_{yx} becomes zero. This reduces (2) to,

$$\left(\mathrm{T}_\mathrm{s}^o\right)^{-1} = \begin{bmatrix} 1 & -\theta_{yz} & \theta_{zy} \\ 0 & 1 & -\theta_{zx} \\ 0 & 0 & 1 \end{bmatrix} \tag{3}$$

To compensate for the bias and scale factor errors, we can model the sensor output as shown in figure 1. This will modify (1) to be,

$$\mathrm{A}^\mathrm{s} = (\mathrm{KT}_\mathrm{s}^o)^{-1}\mathrm{A}^o + \mathrm{B} \tag{4}$$

$$\mathrm{A}^o = \mathrm{KT}_\mathrm{s}^o(\mathrm{A}^\mathrm{s} - \mathrm{B}) \tag{5}$$

Here, K is the diagonal matrix with 3 scale factors k_x, k_y and k_z and B is the column matrix with 3 biases, b_x, b_y and b_z. It should be noted that the measurements from the sensor contain a noise component as well, but since our calibration is not meant to offset the effects of noise, it is not included in the model.

The model in (4) has 9 unknowns: 3 scale factors, 3 misalignment factors and 3 biases.

B. Tri-Axial Gyroscope

Since a MEMS gyroscope suffers from bias, scaling and misalignments errors as well, the above discussion about accelerometer's error model applies to the gyroscope sensor as well. Therefore, a corresponding error model for gyroscope can be obtained in a similar way as,

$$\omega^o = \mathrm{KT}_\mathrm{s}^o\left(\omega^\mathrm{s} - \mathrm{B}\right) \tag{6}$$

Here, ω^o is the gyroscope output in orthogonal body coordinates, ω^s is the measured gyroscope output in sensor coordinates, K is the scale factor and B is the bias.

The above model also has 9 unknowns: 3 scale factors, 3 misalignment factors and 3 biases.

III. Calibration Method

A. Accelerometer's Calibration

The unknown parameters in the accelerometer model are collected to form the vector

$$\mathrm{X} = \left[\, b_x \;\; b_y \;\; b_z \;\; k_x \;\; k_y \;\; k_z \;\; k_{xy} \,\right]^T \tag{7}$$

Where $k_{xy} = \theta_{yz}k_x$, $k_{xz} = (\theta_{yz}\theta_{zx} - \theta_{zy})k_x$ and $k_{yz} = \theta_{zx}k_y$ are misalignment factors obtained by combining K and T_s^o.

Vectors X allows us to define the function h for any k^{th} sensor output such that,

$$\mathrm{A}_\mathrm{k}^o = \mathrm{h}\left(\mathrm{A}_\mathrm{k}^\mathrm{s}, \mathrm{X}\right) = \mathrm{KT}_\mathrm{s}^o(\mathrm{A}_\mathrm{k}^\mathrm{s} - \mathrm{B}) \tag{8}$$

In the case of an accelerometer, ideally the total force measured by it under static conditions should be equal to the local gravity regardless of the orientation of the sensor. Therefore, we can derive a cost function from the error function describing the deviation of the squared magnitude of measured acceleration from the squared magnitude of gravity as,

$$\mathrm{G(X)} = \sum_{K=1}^{L} \left(\left\| \mathrm{h}(\mathrm{A}_\mathrm{k}^\mathrm{s}, \mathrm{X}) \right\|^2 - \left\| \mathrm{g} \right\|^2 \right)^2 \tag{9}$$

Here, the required value of parameter vector $\hat{X}$ is to be obtained as,

$$\hat{X} = \arg\min_X \{\mathrm{G(X)}\} \tag{10}$$

The L in equation (9) is equal to$L = MN$, where N is the number of different orientations sensor is exposed to and M is the number of data samples taken during each particular orientation. If we keep the sensor perfectly static during each orientation, then we can assume that the g force acting on the sensor remains constant at all M samples. This allows us to take the mean of M data samples taken during any particular

k^{th} orientation and use it in (9) to cause the simplification $L = N$ as,

$$\mathrm{G(X)} = \sum_{K=1}^{N} \left(\left\| \mathrm{h}(\overline{\mathrm{A}_{\mathrm{k}}^{\mathrm{s}}}, \mathrm{X}) \right\|^2 - \|\mathrm{g}\|^2 \right)^2 \tag{11}$$

Where $\overline{A_k^s}$ is the mean force measured during a k^{th} orientation. The nonlinear cost function G(X) was minimized using Newton's method with back-tracking, which is,

$$\mathrm{X_k} = \mathrm{X_{k-1}} - \mathrm{t} \frac{\nabla \mathrm{G\,(X)}}{\nabla^2 \mathrm{G\,(X)}} \tag{12}$$

Where X is the unknown parameter vector, $\nabla \mathrm{G\,(X)}$ is the gradient of $\mathrm{G\,(X)}$, $\nabla^2 \mathrm{G\,(X)}$ is the hessian of $\mathrm{G\,(X)}$ and t is the step size which was found by the line search algorithm.

Newton's optimization method is iterative in nature. At each iteration, values of X are calculated to produce a lower value of the cost function than the value calculated from X in the previous iteration. In this way, the function is minimized. The iterations can be stopped when a certain threshold is reached. Details of the method can be found in [15].

1) Initializing X: The function G(X) usually has one or more local minima in addition to a global minimum. To guarantee that the minimization method converges to the global minimum and not to a local minimum, initial value of X should be chosen closer to the value of X at the global minimum. For this purpose, we augmented the calibration method by utilizing a relaxed form of standard 6-position calibration method. We placed the sensor in approximate up-down orientations to estimate the initial biases and scale factors. For each axis, we align the sensor with gravity, collect data and then align it approximately 180 degrees to collect more data. In this way, approximate biases and scale factors can be determined by using individual components of each axis in equation (4) as;

$$k = \frac{a_{up} - a_{down}}{2 \times g} \tag{13}$$

$$b = \frac{a_{up} + a_{down}}{2} \tag{14}$$

Where, k and b is the scale and bias for the corresponding axis with that axis being oriented up and then subsequently down, and a_{up} and a_{down} are the measured acceleration while the sensor is oriented up and down respectively.

B. Gyroscope's Calibration

Similar to the case of an accelerometer, a gyroscope placed on the surface of the earth, does experience earth's rotation rate; which may be used as a reference for calibration purpose as described in [12]. However, for the case of a MEMS gyroscope, the earth's rotation rate signal is too weak to be an effective reference signal as it is buried in large sensor noise.

We propose an alternate method that is not only simple in terms of application and computation but also not dependent on any external equipment and perfect alignments. Compared to a 3-axis sensor formed by mounting 3 individual sensors, the newer single chip multi-axis sensors have relatively small misalignment due to the fact that both the accelerometer and gyroscope are micro machined on a single silicon die. The actual tests done later on, support this idea as the maximum misalignment found was $\theta = 0.0186$ for the case of the accelerometer and only $\theta = 0.0003$ in the case of the gyroscope (Table II and III-B). This makes the scaling factor and bias the most significant error sources and allows (6) to be written as,

$$\omega = \mathrm{K}(\omega^{\mathrm{s}} - \mathrm{B}) \tag{15}$$

The simplest way of determining gyro bias is to keep it in a no-motion state i.e. completely stationary. As we can see from equation (4), ignoring the weak effect of earth's rotation, the sensor output in this state should be equal to bias. This however, automatically assumes that the bias experienced by the sensor during static state is the same as the bias during dynamic state.

Another approach that we consider here is to utilize a scheme for bias and scale factor determination while the sensor is in a dynamic state, so that we can include, if any, the effects of motion on these sensor quantities.

Our first approach is to keep the sensor static for a period of time and then treat the recorded output as bias. Following this, we rotate the sensor around each sensitive axis. In this case, after a rotation has been applied to the sensor and the sensor is once again stationary, the angular change should be,

$$\Delta\theta_{ik} = \overline{\omega_{ik}} T_k \tag{16}$$

Here, i is the active axis and k is the rotation index. So, for any i^{th} axis and k^{th} rotation, $\Delta\theta_{ik}$ is the known angle, $\overline{\omega_{ik}}$ is the average rate measured by the gyroscope and T_k is the elapsed time. The gyroscope provides instantaneous measurements as opposed to average rate; therefore, the mean of the set of gyroscope measurements taken from the total interval was calculated. Using (13), the above equation becomes,

$$\Delta\theta_{ik} = k_i(\overline{\omega_{ik}} - b_i)T_k \tag{17}$$

Using the known value of bias b, we can then calculate the scale k as,

$$k_i = \frac{\Delta\theta_{ik}}{(\overline{\omega_{ik}} - b_i)T_k} \tag{18}$$

Our second approach is to find both bias and scale in a single step. Similar to the previous approach, we rotate the sensor around each sensitive axis, and then from (15), for any i^{th} axis and $k = 1, 2, \ldots n$ rotations, the equation yields a system of n linear equations $\mathrm{Ax} = \mathrm{b}$, with

$$\mathrm{A} = \begin{bmatrix} \overline{\omega_{i1}} T_1 & -T_1 \\ \vdots & \vdots \\ \overline{\omega_{in}} T_n & -T_n \end{bmatrix}, \quad \mathrm{x} = \begin{bmatrix} k_i \\ k_i b_i \end{bmatrix} \;\&\; \mathrm{b} = \begin{bmatrix} \Delta\theta_{i1} \\ \vdots \\ \Delta\theta_{in} \end{bmatrix} \tag{19}$$

Since there are two unknowns, only 2 equations are needed to solve (17); however, considering the case $n > 2$, for a more confident solution, (17) results in an over determined system without a unique solution. Our approach in this scenario is to find the solution using the least squares method as,

$$\hat{X} = \arg\min_{X} \{\mathrm{G(x)}\} \tag{20}$$

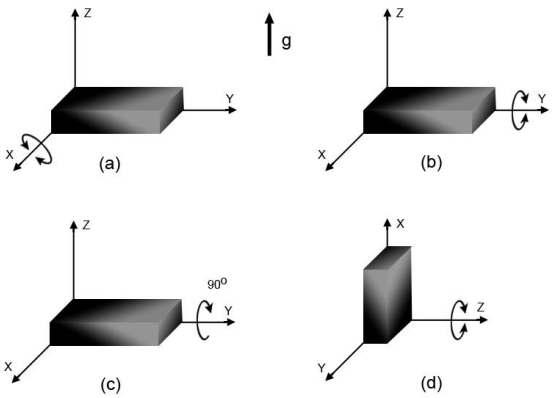

Fig. 2. Rotations needed to determine calibration parameters. (a) For x axis. (b) For y axis. (c) and (d) For z axis. (g is gravity's orientation.)

Where $G(x) = \|e(X)\|^2$ and e(x) is the residual error $e(x) = Ax - b$.

It can be shown that the solution $\hat{X}$ which minimizes the residual can be obtained by solving,

$$A^T Ax = A^T b \tag{21}$$

for x. Proof of the above can be found in [16]. Further, to avoid any confusion, we will refer the first approach as Static Bias approach and the second approach as Dynamic approach.

To apply this procedure, information about the known angle is required. In our case, since the accelerometer and gyroscope are on a single die, any rotation experienced by one sensor will equally be experienced by the other sensor as well. Therefore, the accelerometer already calibrated from the method of the previous section can easily measure change of angle around each individual axis. The complete method with equations for this scheme is described in the appendix. Further, the accelerometer utilizes gravity to detect rotations, i.e., if placed horizontally with its z axis aligned with gravity, it can measure rotation around x axis and y axis. Since, it is insensitive to movements around gravity; rotations around z axis cannot be measured in the same coordinate axes. To overcome this limitation, we rotate the coordinate axes first 90 degrees around y axis and then follow the same procedure by swapping z-axis with y-axis. Figure 2 shows the sequence of rotations needed to solve for all the three axes.

With this method, the gyroscope can be calibrated easily with rotations performed approximately around each sensitive axis. No special angle of rotation is required. Any combination of rotations within the range of $\pm 180°$ can be used.

IV. Experimental Results

To evaluate the performance of the proposed calibration method, experiments were carried out on a custom made IMU. Section IV-A describes the experimental setup, section IV-B contains the accelerometer's calibration results and section IV-C describes the gyroscope's calibration results.

A. Experimental Setup

1) Custom Built IMU: A wireless IMU was built for the experiments as shown in figure 3. Table I gives the significant specifications of the IMU. The IMU was built using the BNO055 sensor from Bosch which contains a tri-axial accelerometer, gyroscope and a magnetometer on a single chip. Details can be found in the datasheet [16].

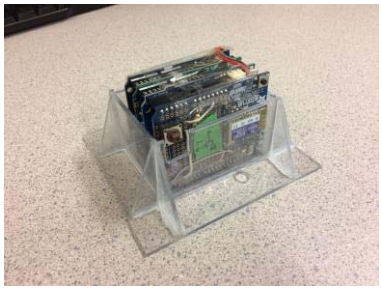

Fig. 3. Custom made wireless IMU based on Bosh BNO055 sensor.

TABLE I
Significant Features of IMU

Feature	Detail
Microcontroller	ATSAMD21 ARM Cortex M0 +
Sensor	Bosh BNO055
Communication	Serial + Bluetooth
Sampling Rate	100 Hz

Fig. 4. Xsens Mti-G710 commercial IMU.

2) Xsens MTi-G710 Commercial IMU: Shown in figure 4, the MTi-G710 is a commercial IMU by Xsens, primarily designed for industrial applications. It is delivered with factory calibration data which will serve as a benchmark to test against our proposed method. Complete details about the sensor can be found in the datasheet [17].

B. Calibration of Custom Built IMU

1) Accelerometer's Calibration: The first step is to determine the initial X vector of equation (12) as described by equation (13) and (14) and the discussion

preceding them. We found the vector to be,

$$X = \begin{bmatrix} 0.06 & -0.14 & -0.11 & 9.86 & 9.88 & 9.63 & 0 & 0 & 0 \end{bmatrix}^T$$

Following this, 10 sets of data were recorded. Each set was comprised of 18 measurements obtained from placing the sensors in 18 different orientations. Out of these 18, 6 orientations correspond to the 6 faces of a cube and 12 correspond to 12 edges (sensor was aligned on the edges at 45° from the faces). During each orientation, 2 seconds of data or 200 samples equivalently were taken to counter the effects of noise while the sensor was kept stationary.

TABLE II
AVERAGE CALIBRATION PARAMETERS OF ACCELEROMETER FOUND WITH 10 SETS OF DATA

PARAMETER	VALUE	
	Mean	*Standard Deviation*
$b_x(g)$	0.0097	0.0004
$b_y(g)$	-0.0367	0.0035
$b_z(g)$	-0.0101	0.0007
k_x	1.0061	0.0001
k_y	1.0067	0.0004
k_z	0.9831	0.0002
k_{xy}	-0.0122	0.0005
k_{xz}	0.0188	0.0006
k_{yz}	0.0005	0.0005

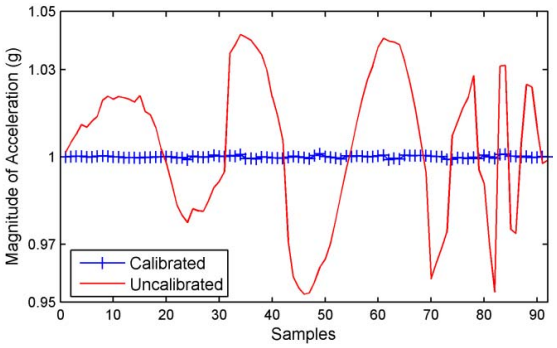

Fig. 5. Magnitude of calibrated acceleration vs. un-calibrated raw acceleration. Calibrated output has smaller variance than raw output.

Calibration parameters were obtained by running the calibration method on each set and then the mean were taken, which is reported in table II. The calibration method managed to converge in under 10 iterations.

To analyze the effect of calibration, the sensor was placed in 92 different orientations and the data was compensated by the calibration parameters of table II. A graphical representation is shown in figure 5. The effect of calibration is evident as the magnitude is much closer to the value of 1g, with the RMS (Root Mean Square) error decreasing from 0.0129 to 0.0014, and standard deviation from 0.0128 to 0.0014. This is a reduction in RMS error by a factor of 9.

2) Gyroscope's Calibration: To calibrate the gyroscope, 15 sets of data were recorded with 5 sets for each axis. Each set was comprised of 18 rotations.

The rotations were applied by hand, as described in figure 2 for each axis and each of the 18 rotations were different than the other. In order to avoid jerks in motion that might push the rate outside of the measurable range of the gyro, the rotations were applied as smooth as possible. The sensor was kept stationary for at least 5 seconds or 500 samples both before and after a rotation was applied and average values were taken to remove the noise effects. Table III-A reports the mean calibration parameters obtained by the static bias approach and dynamic approach.

The results of the proposed calibration method were compared with the calibration method described in [10] and [11], which is based on using a single axis motion rate table to acquire the reference signal. The rate table utilized in our experiments is from Ideal Aerosmith, model 1621, which has a rate accuracy of $\pm 0.01\%$. The rate table is shown in figure 6.

Fig. 6. Single axis rate table by ideal Aerosmith.

To calibrate the sensor with the rate table, the IMU was placed in 18 different configurations. Out of these 18, 6 configurations correspond to the 6 faces of a cube and 12 correspond to 12 edges (sensor was aligned on the edges at 45° (approx.) from the faces). Since the rate table can apply both clockwise and counter-clock wise rates, only 9 different orientations were required.

The proposed method is based on rotations which involve acceleration and deceleration. In other words, the rate will start from zero, reach a maximum value and then go back to zero. Because the rotations are applied by hand, the rate will probably not increase or decrease monotonically; however, this is not a requirement and it doesn't affect the calibration. On the other hand, the calibration achieved by the rate table utilizes constant rate. Therefore, to achieve a proper comparison, the sensor was calibrated by using the rate table over different rates up to 150 $^\circ/s$. Subsequently, the rotations needed for the proposed method were also carefully applied (by hand) to not exceed the 150 $^\circ/s$ range. It should be noted that this is not a requirement for calibration but it was only done for the sake of comparison.

Table III-B shows the calibration parameters obtained by the rate table and the corresponding deviation error (%) of parameters determine by the two proposed approaches. It was observed that the methods agree very well. The overall mean error in both the cases was less than 0.41 %. Some of the individual parameter errors were larger in the static case and smaller in the dynamic case and some were vice versa The static approach overall did produce slightly better results than the dynamic approach; however, the difference in not significant.

C. Calibration of Xsens Mti-G710

1) Accelerometer Calibration: In this experiment, the same approach was used to calibrate the Xsens IMU as it was used to calibrate the custom built IMU. The initial X vector was found to be,

$$\mathrm{X} = \begin{bmatrix} 32721 & 32731 & 32744 & 133 & 134 & 135 & 0 & 0 & 0 \end{bmatrix}^T$$

Following this, the rest of the procedure was applied and the method converged in under 10 iterations. Table IV-A reports the parameters found, while Table IV-B reports the factory calibration parameters with corresponding deviation error from the calculated parameters.

TABLE III

(A) AVERAGE CALIBRATION PARAMETERS OF GYROSCOPE FOUND WITH 5 SETS OF DATA FOR EACH AXIS. (B) AVERAGE CALIBRATION PARAMETERS FOUND USING THE RATE TABLE WITH CORRESPONDING DEVIATION ERROR

(A)

PARAMETER	STATIC APPROACH		DYNAMIC APPROACH	
	VALUE		VALUE	
	Mean	*Standard Deviation*	*Mean*	*Standard Deviation*
$b_x(°/s)$	-0.0482	0.0040	-0.0480	0.0074
$b_y(°/s)$	0.0644	0.0022	0.0643	0.0053
$b_z(°/s)$	0.0554	0.0033	0.0544	0.0068
k_x	0.9754	0.0042	0.9777	0.0011
k_y	0.9830	0.0016	0.9829	0.0005
k_z	0.9747	0.0041	0.9638	0.0026

(B)

PARAMETER	VALUE		DEVIATION ERROR FROM MEAN VALUE (%)	
	Mean	*Standard Deviation*	*Static Approach*	*Dynamic Approach*
$b_x(°/s)$	-0.0484	0.0031	0.4132	0.8264
$b_y(°/s)$	0.0640	0.0067	0.6250	0.4687
$b_z(°/s)$	0.0549	0.0049	0.9107	0.9107
k_x	0.9770	0.0005	0.1638	0.0716
k_y	0.9822	0.0005	0.0814	0.0713
k_z	0.9766	0.0005	0.1946	1.3107
k_{xy}	-0.0002	0.0002	-	-
k_{xz}	0.0004	0.0002	-	-
k_{yz}	0.0003	0.0002	-	-
Mean Error	-	-	0.1409	0.4060
Max Error	-	-	0.9107	1.3107

The deviation error of misalignments was not calculated because due to the difference in sensor models, there is no basis for a direct comparison. The Xsens uses a 12-parameter model whereas we use a 9-parameter model for simplicity. This however, doesn't impact the derived accuracy, which was confirmed by the magnitude based tests. In this experiment, the sensor was placed in 90 different orientations as before and the data was compensated by the calculated calibration parameters of table IV-A along with the factory parameters of Table IV-B. The result is shown in figure 7.

It can be seen that the calculated parameters performed better than the output produced by factory calibration. The RMS error, in this case, reduced from 0.130 to 0.011 and the standard deviation reduced from 0.131 to 0.011.

2) Gyroscope Calibration: Similar approach was applied to the Xsens gyro for calibration as applied to the custom built IMU. Table V-A reports the calibration parameters found by the static and dynamic approach.

The factory calibration parameters are reported in Table V-B along with the corresponding deviation error for each parameter calculated by the proposed method.

It was once again observed that the parameters found agree very well with the factory given calibration values, with the overall mean error being less than 0.219 % in both the static and dynamic cases. The overall error for both the cases was also almost identical. In light of these results, the choice of applying the static or dynamic approach becomes much more of a preference than to obtain a significant difference in accuracy between the two. A notable difference, however, might be observed if the dynamic bias is significantly different than the static bias. In this case, the dynamic method will produce a result that is closer to reality as it produces the best fit of all the data collected in the calibration window.

TABLE IV

(A) AVERAGE CALIBRATION PARAMETERS OF ACCELEROMETER FOUND WITH 10 SETS OF DATA. (B) FACTORY CALIBRATION DATA FOR THE IMU'S ACCELEROMETER WITH CORRESPONDING DEVIATION ERROR

(A)

PARAMETER	VALUE	
	Mean	*Standard Deviation*
$b_x(m/s^2)$	32720.62	1.4876
$b_y(m/s^2)$	32733.77	1.8070
$b_z(m/s^2)$	32741.15	1.2540
k_x	133.48	0.0364
k_y	134.28	0.0569
k_z	135.61	0.0077
k_{xy}	0.21	0.0342
k_{xz}	2.84	0.0361
k_{yz}	-0.63	0.0414

(B)

PARAMETER	VALUE	DEVIATION ERROR FROM MEAN VALUE (%)
	Mean	
$b_x(m/s^2)$	32721.4	0.0024
$b_y(m/s^2)$	32739.6	0.0178
$b_z(m/s^2)$	32769.7	0.0871
k_x	133.93	0.3360
k_y	134.11	0.1268
k_z	135.38	0.1699
k_{xy}	0.1332	-
k_{xz}	1.0660	-
k_{yz}	-1.5690	-
Mean Error	-	0.123
Max Error	-	0.3360

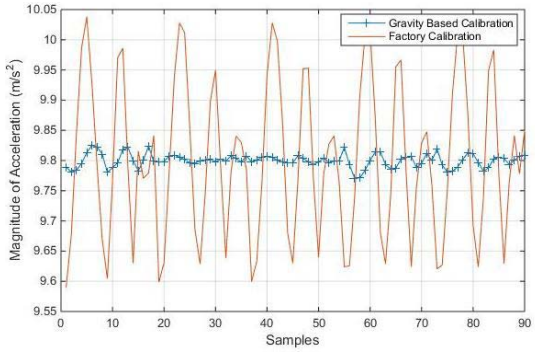

Fig. 7. Magnitude of calibrated acceleration vs. calibration by factory parameters. Gravity based calibrated output has smaller variance than factory output.

TABLE V
(A) AVERAGE CALIBRATION PARAMETERS OF GYROSCOPE FOUND WITH 5 SETS OF DATA FOR EACH AXIS. (B) FACTORY CALIBRATION DATA FOR THE IMU'S GYROSCOPE

(A)

PARAMETER	STATIC APPROACH		DYNAMIC APPROACH	
	VALUE		VALUE	
	Mean	*Standard Deviation*	*Mean*	*Standard Deviation*
$b_x(rad/s)$	32998.43	8.488	32998.96	7.729
$b_y(rad/s)$	32176.06	1.5836	32176.61	1.5838
$b_z(rad/s)$	32907.26	0.4763	32906.34	0.5956
k_x	3206.91	32.713	3155.18	35.388
k_y	3290.33	5.8142	3295.35	21.9920
k_z	3130.43	15.43	3153.62	19.2145

(B)

PARAMETER	FACTORY VALUE	DEVIATION ERROR FROM MEAN VALUE (%)	
	-	*Static Approach*	*Dynamic Approach*
$b_x(rad/s)$	32998.5	0.0001	0.0013
$b_y(rad/s)$	32193.8	0.0551	0.0534
$b_z(rad/s)$	32905.9	0.0041	0.0013
k_x	3181.57	0.7966	0.8292
k_y	3298.56	0.2495	0.0973
k_z	3142.16	0.3733	0.3647
Mean Error	-	0.2182	0.2160
Max Error	-	0.7966	0.8292

Further, if the deviation is large over time, it would be better to recalibrate the sensor for better accuracy.

V. CONCLUSION

This paper explored the in-field calibration of a MEMS IMU with the objective of devising a calibration algorithm that does not require any external equipment and can be performed in-field, in non-laboratory conditions. With the application of the proposed method, any IMU can be easily calibrated in-field with just a few simple rotations in under 20 minutes. The method presented requires only earth's gravitation field as a reference to perform calibration and eliminates constraints on sensor's orientation during calibration. The experimental results obtained through a custom-built IMU, a commercial IMU and an aviation grade rate table conform the validity of the proposed method.

While eliminating the need of external equipment, as in the case of traditional methods, the algorithm still requires the IMU under test to be accessible to apply the proposed rotations. This might prevent recalibration if the structure to which it is fixed to, doesn't allow movements. A recommended solution to this issue is to design modular systems, so that an IMU can be plugged in and out easily for calibration.

It is evident from the results that because of simplicity and no additional cost, the method is quite useful for developers to calibrate a MEMS IMU for low cost applications, without needing external equipment such as a turn table and with no further need to mount the sensors in perfect alignments.

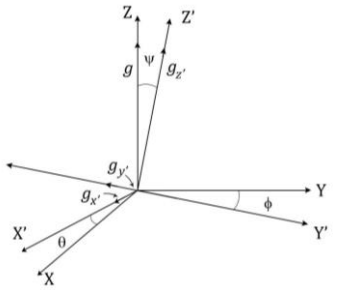

Fig. 8. Coordinate axes < X, Y, Z > and < X', Y', Z' >.

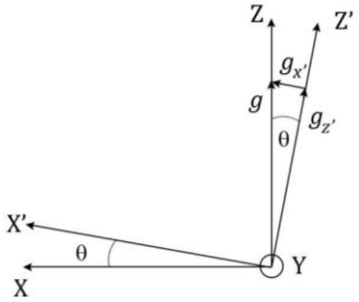

Fig. 9. Side view of motion around Y axis.

APPENDIX
CALCULATION OF TILT ANGLES FROM THE ACCELEROMETER

We begin by placing an accelerometer on the surface of the earth. Considering that the accelerometer is static, the only force acting on it is the gravity. Therefore, regardless of the orientation of the sensor, the magnitude of the acceleration measured by a 3-axis accelerometer is equal to acceleration due to gravity (g).

We define an orthogonal coordinates axes < X, Y, Z > in which the gravity vector aligns with the Z axis. We also define body axis < X', Y', Z' > which is attached to the sensor as shown in figure 8.

From figure 8, we see that,

$$g_{X'}^2 + g_{Y'}^2 + g_{Z'}^2 = g^2 \tag{22}$$

First, we will consider the rotation θ around the Y axis. Looking at the coordinate axis from the Y axis in figure 8, we construct figure 9. From the geometry we can see that,

$$\tan\theta = \frac{g_{X'}}{g_{Z'}} \tag{23}$$

Now, consider angle ϕ obtained by the motion around X axis. The geometry is show in figure 10.

We can see from the figure that,

$$\tan\phi = \frac{g_{Y'}}{g_{Z'}} \tag{24}$$

Now consider the case of combined rotation, where the rotation of ϕ is applied after a rotation of θ as shown in figure 11. This results in the component $g_{Z'}$ on the Z axis to decrease in length. As we can see from (23), the value of $\tan\theta$ will increase; however, in reality, the actual angle θ remained changed. We also notice that by this second rotation, the component $g_{Y'}$ on the Y axis will start to increase in length by the same amount the component $g_{Z'}$ on the Z axis decreases.

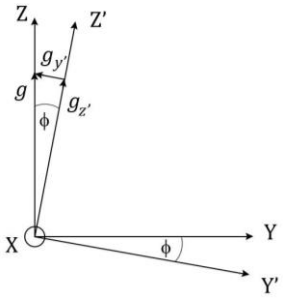

Fig. 10. Side view of motion around X axis.

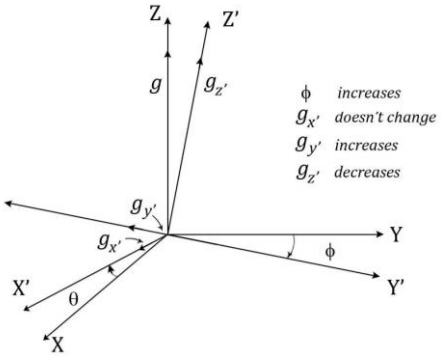

Fig. 11. Rotation around X and Y axes.

Therefore, equation (21) needs to be modified as;

$$\tan\theta = \frac{g_{X'}}{\sqrt{gZ'^2 + gY'^2}} \tag{25}$$

Similarly, equation (21) becomes;

$$\tan\phi = \frac{g_{Y'}}{\sqrt{g_{Z'}^2 + g_{X'}^2}} \tag{26}$$

Also, by using (22) we can write these equations as;

$$\tan\theta = \frac{g_{X'}}{\sqrt{g^2 - g_{X'}^2}} \tag{27}$$

and

$$\tan\phi = \frac{g_{Y'}}{\sqrt{g^2 - g_{Y'}^2}} \tag{28}$$

The above equations can be used to calculate tilt from the accelerometer once it has been calibrated. It should be noted that these equations are valid for independent rotations occurring without following a specific sequence. Combined rotations occurring in a sequence, such as, represented by Euler angles, require a modified form of the above equations depending on the order in which the rotations were applied.

ACKNOWLEDGMENT

The authors would like to thank Dr. Ed Park's team for providing the Xsens Sensor.

REFERENCES

[1] M. Park and Y. Gao, "Error and performance analysis of MEMS-based inertial sensors with a Low-cost GPS receiver," *Sensors*, vol. 8, no. 4, pp. 2240–2261, 2008.

[2] C. Lukianto, C. Hönniger, and H. Sternberg, "Pedestrian smartphone-based indoor navigation using ultra portable sensory equipment," in *Proc. Int. Conf. Indoor Positioning Indoor Navigat. (IPIN)*, Zurich, Switzerland, Sep. 2010, pp. 15–17.

[3] H. J. Luinge and P. H. Veltink, "Measuring orientation of human body segments using miniature gyroscopes and accelerometers," *Med. Biol. Eng. Comput.*, vol. 43, no. 2, pp. 273–282, Mar. 2005.

[4] A. Y. Benbasat and J. A. Paradiso, "An inertial measurement framework for gesture recognition and applications," in *Proc. Int. Workshop Gesture Sign Lang. Hum.-Comput. Interact.*, London, U.K., 2001, pp. 9–20.

[5] J.-S. Wang, Y.-L. Hsu, and J.-N. Liu, "An inertial-measurement-unit-based pen with a trajectory reconstruction algorithm and its applications," *IEEE Trans. Ind. Electron.*, vol. 57, no. 10, pp. 3508–3521, Oct. 2010.

[6] A. D. Cheok, K. G. Kumar, and S. Prince, "Micro-accelerometer based hardware interfaces for wearable computer mixed reality applications," in *Proc. 6th Int. Symp. Wearable Comput.*, Seattle, WA, USA, Oct. 2002, pp. 223–230.

[7] A. B. Chatfield, *Fundamentals of High Accuracy Inertial Navigation*. Washington, DC, USA: AIAA, 1997.

[8] D. H. Titterton and J. L. Weston, *Strapdown Inertial Navigation Technology*, 2nd ed. Washington, DC, USA: AIAA, 2004, ch. 8.

[9] F. Ferraris, U. Grimaldi, and M. Parvis, "Procedure for effortless in-field calibration of three-axis rate gyros and accelerometers," *Sens. Mater.*, vol. 7, no. 5, pp. 311–330, 1995.

[10] I. Skog and P. Händel, "Calibration of a MEMS inertial measurement unit," in *Proc. 18th IMEKO World Congr.*, Rio de Janeiro, Brazil, Sep. 2006, pp. 1–6.

[11] Z. F. Syed, P. Aggarwal, C. Goodall, X. Niu, and N. El-Sheimy, "A new multi-position calibration method for MEMS inertial navigation systems," *Meas. Sci. Technol.*, vol. 18, no. 7, pp. 1897–1907, 2007.

[12] E. H. Shin and N. El-Sheimy, "A new calibration method for strapdown inertial navigation systems," *Z. Vermess*, vol. 127, pp. 41–50, Jan. 2002.

[13] D. Jurman, M. Jankovec, R. Kamnik, and M. Topič, "Calibration and data fusion solution for the miniature attitude and heading reference system," *Sens. Actuators A, Phys.*, vol. 138, no. 2, pp. 411–420, 2007.

[14] G. Olivares, A. Olivares, J. M. Górriz, and J. Ramírez, "High-efficiency low-cost accelerometer-aided gyroscope calibration," in *Proc. IEEE Int. Conf. Test Meas.*, Hong Kong, Dec. 2009, pp. 354–360.

[15] L. Vandenberghe and S. Boyd. (2011). *Notes on Applied Numerical Computing*. [Online]. Available: http://www.ee.ucla.edu/~vandenbe/103/reader.pdf

[16] Bosch Sensortech. (2016). *BNO055 Intelligent 9-Axis Absolute Orientation Sensor*. [Online]. Available: http://ae-bst.resource.bosch.com/media/_tech/media/datasheets/BST_BNO055_DS000_14.pdf

[17] *Xsens MTi 100-Series: The Most Accurate and Complete MEMS Based IMU, VRU, AHRS and GNSS/INS*. Accessed: Feb. 2017. [Online]. Available: https://www.xsens.com/download/pdf/documentation/mti-100/mti-100-series.pdf

Umar Qureshi received the B.E. degree from the Department of Electronic Engineering, DCET, Karachi, Pakistan, in 2012. He is currently pursuing the M.A.Sc. degree with the School of Mechatronic Systems Engineering, Simon Fraser University, BC, Canada.

His research interest includes inertial sensors, calibration and error reduction, Kalman filters, and head motion analysis.

Farid Golnaraghi received the B.S. and M.S. degrees in mechanical engineering from the Worcester Polytechnic Institute, Worcester, MA, both in 1982, and the Ph.D. degree in theoretical and applied mechanics from Cornell University, Ithaca, NY, in 1988.

In 1988, he became a Professor of Mechanical Engineering, and then a Professor of Mechanical and Mechatronics Engineering with the University of Waterloo, Waterloo, ON, Canada. He also became a Tier I Canada Research Chair in mechatronics and smart material systems at Waterloo in 2002. In 2006, he became the Director of the Mechatronics Engineering Program with Simon Fraser University, Surrey, BC, Canada. He is currently the Burnaby Mountain Endowed Chair. Over the past 27 years in Waterloo and SFU, he has been very active in the supervision of graduate students. His pioneering research has resulted in two textbooks, more than a hundred papers, four patents, and two start-up companies.